

MELTING BEHAVIOR OF COAL ASH MATERIALS FROM COAL ASH COMPOSITION

by

Karl S. Vorres
Institute of Gas Technology
Chicago, Illinois 60616

May 1977

INTRODUCTION

The melting behavior of coal ash materials is characterized by several temperatures relating to stages of deformation of cone-shaped ash samples on heating. Viscosity of coal ash melts through the molten temperature range is also useful for characterization. This information has been used primarily for design of steam generation equipment, but may be usefully extended to coal conversion processes such as gasification. Coal ash does not melt sharply like a pure compound, but rather softens over a temperature range as the temperature is increased. As it melts, the heated ash exhibits a plastic range between the solid and mobile liquid states. The temperature range corresponding to the plastic state, as well as viscosity and melting phenomena, depend on the composition of the ash and the gaseous environment. Studies of the melting and viscosity of ash melts over a range of temperatures and gaseous environments have demonstrated this dependence.^{1,2,3}

The purpose of this paper is to provide some framework for understanding the observed behavior, and to suggest use of a concept that should be helpful in further studies of that behavior.

Acids and Bases

The melting and viscosity behavior has been described as a function of the composition of the coal ash in terms of acids and bases. The acids have been defined as oxides of Al, Si, and Ti, while the bases were oxides of Na, K, Ca, Mg, and Fe.

The structural inorganic chemical characteristics of the acids and bases will be of interest in establishing the reasons for labels such as acid or base, and in understanding the impact of the acid or base characteristics on the melting or viscosity properties of coal ash.

Inorganic cations may be characterized by ionic radii for their common valences. In general, the radii decrease with charge, and also with atomic weight for a given valence. The radii, according to Ahrens, for the inorganic cations indicated above are listed below in Angstrom units:

Si ⁺⁴	0.42	Fe ⁺²	0.74
Al ⁺³	0.51	Na ⁺¹	0.94
Fe ⁺³	0.64	Ca ⁺²	0.99
Mg ⁺²	0.67	K ⁺¹	1.33
Ti ⁺⁴	0.68		

The two values are given for iron because of the importance of both valence states.

In crystals, and in some cases for liquids, the cations are surrounded by a specific number of anions. This coordination number is determined by the ratio of the radii of the two oppositely charged species. A coordination number of four produces a tetrahedron and is expected between radius ratio limits of 0.225 and 0.414. A coordination number of six produces an octahedron and is expected between radius ratio limits of 0.414 and 0.732. The coordination number of eight is expected for somewhat larger radius ratios.

In coal ash the predominant anion is the oxide ion. Using a radius of 1.40 Å for the oxide and applying the radius ratio criteria, tetrahedral coordination is expected for cations with a radius smaller than 0.58 Å or specifically Si⁺⁴ and Al⁺³. The octahedral configuration is expected for cations between 0.58 and 1.03 Å or Fe⁺³, Mg⁺², Ti⁺⁴, Fe⁺², Na⁺¹, and Ca⁺². The remaining K⁺¹ would be expected to have a cubic configuration with coordination number eight. Under proper conditions, these coordination numbers would be expected in melts.

Ionic Potential

Another useful concept is the ionic potential which is defined as the quotient of the valence and ionic radius for a given ion. This parameter indicates something about the ability of a cation to coordinate anions about it. A higher ionic potential indicates the ability of one cation type to compete effectively with other cations for available anions to form complex ions such as SiO_4^{-4} in a mixture like coal ash. The values for the ionic potentials of the species of interest are:

Si ⁺⁴	9.52	Fe ⁺²	2.70
Al ⁺³	5.88	Ca ⁺²	2.02
Ti ⁺⁴	5.88	Na ⁺¹	1.06
Fe ⁺³	4.69	K ⁺¹	0.752
Mg ⁺²	2.98		

The highest values belong to the acid group Si, Al, and Ti, while the lowest values belong to the bases.

It is suggested here that the ionic potential may be the physical characteristic which is useful in quantifying acid and base behavior, and would also be useful in future efforts to correlate melting behavior or viscosity with chemical composition.

The ionic potential is a measure of a cation's ability to compete for anions in order to form a complex ion of the form MO_x^{-n} . The ability is also dependent on the available oxide ions. The ability of Si to coordinate four oxide ions would be limited in the pure oxide SiO_2 if it were not for the possibility of sharing oxide ions between different Si. As a result, repeating SiO_2 groups in a V shape can form polymer type groupings. These groupings could be extremely long chains of linked tetrahedra. Other forms are also possible. If additional oxide ions became available, then they would provide the species needed to terminate the chains. As more oxide became available, the groupings would terminate more frequently and have a smaller agglomerate weight. A source for oxide ions would be oxides of cations with low ionic potential such as the alkalis or alkaline earths. These would be expected to dissociate into hard sphere ions, and the oxide ions would be coordinated by cations of the highest ionic potential.

It is suggested that the role of acids in coal ash melts is that of polymer formers with the greatest tendency to form polymers correlating with the greatest ionic potential. The role of bases is that of oxide ion donors. The oxide ions would be attracted to the ions of high potential to break up polymers and reduce viscosity.

In general, the available oxide ions from cations would tend to reduce the size of polymeric groups associated with cations of high ionic potential. Additions of compounds increasing the available oxide ion concentration would decrease the viscosity of a melt rich in Si and Al typical of eastern coal ash material. This effect has already been noted.

The Behavior of Iron

The two valence states of iron give significantly different values with the ferric ion being between the two groups. The special importance of iron can, in part at least, be correlated with the two valences it displays. This may be compared with the amphoteric behavior of certain other species. On the basis of the table of ionic potentials, the ferric ion may be thought of as a weak acid, and the ferrous ion as a base. In practice, the iron in coal ash in boilers will exist as a mixture of the two states. Only a minor part, frequently about 20%, is Fe_2O_3 . The major part (about 80%) is FeO , with possibly some elemental iron. This indicates the appropriateness of classifying iron oxides (if they must be lumped into one type) with the bases, even though they are listed as Fe_2O_3 .

The gaseous environment is important in determining properties of coal ash systems. Studies have shown a marked reduction of viscosity of melts in going from oxidizing to reducing conditions, which would significantly alter the proportion of ferric and ferrous ions. This change in properties would be consistent with a complex ion forming tendency for the ferric ion with its high ionic potential, and an oxide ion donor role for the ferrous ion with its lower ionic potential. Two factors would work to reduce the viscosity in a reducing environment: 1) reduction of concentration of polymer forming ferric ions, and 2) increase in oxide ion concentration available for cations with high ionic potential. The oxide ions would have been associated with the ferrous ions.

Conceptual Structural Considerations

Winegartner and Rhodes³ indicated that the coefficients in front of the bases CaO, MgO, K₂O, and Na₂O should each be one when calculating the softening temperature using the base-to-acid ratio and expressing the ash composition for these materials in mole percentages rather than weight percentages. The implication of that observation in the context of this paper is that the bases are equally effective as oxide ion donors. Each formula contains one oxide unit. They further note that Fe₂O₃ should really be expressed as FeO. This is also consistent with characterizing FeO as a base and indicating the role of oxide ion donor for FeO.

The melting process may be pictured as application of energy to disrupt the crystal lattice of a solid. The lattice of the solid may be modified by the impurities to permit easier melting through introduction of additional large oxide ions in the acid oxide structure. Insertion of base cations would probably occur in the available interstices appropriate for the base coordination number. The resultant lattice strain would yield a lower thermal requirement for melting or a lower melting point. The further implication of Winegartner and Rhodes work is that the number of oxide ions is most significant, and that the nature of the base cations is not significant in affecting the softening temperature.

SUMMARY

The ionic potential (valence divided by ionic radius) may be used as a measure of acids and bases in predicting coal ash melting and viscosity from the chemical composition. The role of an acid is that of a complex ion former with anions provided by bases which in coal ash systems are oxide ion donors. In systems containing acids and limited oxide ion concentrations, polymers tend to form in the melts. Addition of bases reduces polymer size and would decrease viscosity. The gaseous environment may alter the relative concentration of ferric and ferrous ions, interconverting acid and base ions. In general, bases are reported to be equally effective oxide ion donors. The effects of base addition are proportional to the amount of oxide ion provided to the system.

REFERENCES CITED

1. Sage, W. L. and McIlroy, J. B., J. Engineering for Power, 82, 145 (1960).
2. Rees, O. W., III. State Geological Survey, Circular 365 (1964).
3. Winegartner, E. C. and Rhodes, J. Engineering for Power, 97, 395 (1975).

CHARACTERISTICS OF ASH AGGLOMERATES FROM AN ASH-AGGLOMERATING GASIFIER

David M. Mason

Institute of Gas Technology
3424 S. State Street
Chicago, Illinois 60616

INTRODUCTION

An ash-agglomerating fluidized-bed gasifier has been under investigation at the Institute of Gas Technology (IGT). In such a process, carbon utilization can be substantially improved over that obtained when ash is removed by continually discharging a nonselective portion of the fluidized bed containing both ash and carbon.

The pilot plant gasifier has a diameter of 4 feet and operates at near atmospheric pressure. The schematic diagram of Figure 1 shows that agglomerated ash leaves the gasifier through a centrally located venturi tube through which part of the gaseous feed (steam plus air or oxygen) is introduced to the reactor. Details of the gasifier and its operation have been described by Sandstrom, Rehmat, and Bair in a recent paper (8). In the present paper, we describe the agglomerated ash obtained during gasification of coke breeze and FMC char, and we discuss the probable mechanisms of their formation.

EXPERIMENTAL

Petrographic samples were mounted, sectioned, and polished mostly according to methods employed in coal petrography (1). Our apparatus for microscopical observations and determination of reflectance has been described (4).

Iron oxides and sulfides can usually be recognized by appearance, especially when more than one oxide or sulfide is present. Ferrous sulfide is brilliant, though not as brilliant as pyrite, and has a yellowish cast. Ferrous oxide is dead white, while magnetite is darker and gray in color. In initial observations and if doubt is aroused, measurement of reflectance is useful. Reflectance in air is used in ore petrography. Our own approximate measurements with oil immersion, arranged in order of increasing reflectance, are shown below, together with literature values for reflectance in air. Values for some of the compounds can vary with orientation and composition.

<u>Mineral or Compound</u>	<u>Formula</u>	<u>Reflectance</u>	
		<u>In Air (3)</u>	<u>In Oil (Approx)</u>
		%	
Iron Spinel	FeO·Al ₂ O ₃	--	0.9-1.2
Magnetite	Fe ₃ O ₄	21.1	7-8
Ferrous Oxide	Fe _{1-x} O	--	18-24
Ferrous Sulfide	Fe _{1-x} S	42	18-24
Pyrite	FeS ₂	54.5	33-44
Iron Metal	Fe	--	40-50

Scanning electron microscopy was carried out under the direction of Dr. Oom Johari at IIT Research Institute.

Ash samples were analyzed by the lithium borate fusion method of Boar and Ingram (2), with aluminum, calcium, iron, silicon, and titanium finished by atomic absorption and with sodium and potassium by flame emission. Sulfate was determined by the Eschka method. Acid-soluble iron was extracted by boiling with 3N hydrochloric acid and was determined by atomic absorption.

Agglomerated Ash From Coke Breeze

The ash product consisted predominantly of well-rounded particles (beads) ranging from about 1/16 to 1/4 inch in diameter, sometimes accompanied by some angular coke particles (Figure 2a).

Beads from an early run (No. 17) were subjected to detailed examination. The air-to-steam ratio in this test was about 4:1 by weight; temperature in the fluidized bed ranged from about 1880^o to 1930^oF.

For microscopic observation the beads were mounted in epoxy resin, sectioned, and polished. A composite photomicrograph of a whole 1-inch briquet, taken with vertical illumination, is shown in Figure 3. Residual coke appears as light areas here, both as the main constituent of the angular particles and as the very small constituent particles of the rounded beads. These small particles are situated mostly on the periphery of the beads, although a few are buried in the interior.

The many rounded black areas in the bead are empty vesicles. Others, connected by passageways to the exterior, were filled with the epoxy resin during mounting. (The system is evacuated before covering the sample with the resin, and the liquid resin is forced into some of the vesicles by the readmitted atmospheric pressure.)

A composite photomicrograph of the same briquet taken with oblique illumination is shown in Figure 4. With this illumination, the continuous phase of glassy, melted ash in the rounded beads can be distinguished from many of the embedded, unmelted particles.

We did not attempt to identify all of the unmelted ash particles; however, we think that some with high reflectance are probably particles of high-alumina refractory from the walls of the unit. When the reflectances of some of these high-reflectance particles were measured, they agreed with that of the similarly mounted refractory. Very small vesicles in the melted ash appear as pinpoints of reflected light. Some of the large, empty vesicles are partly illuminated on one side.

The distribution of the residual carbon indicated by microscopic observation was substantiated by further investigation: A sample of the residue was separated by hand into beads and angular particles; analyses for carbon then showed only 1.9 weight percent in the beads and 70.4 weight percent in the angular particles. That most of the residual carbon in the beads is not embedded and is available for reaction was shown by igniting a sample of the beads for 1/2 hour at about 1550^oF, followed by an analysis for unburned carbon. Only 0.36 weight percent remained.

The surface energy of a melt (or solid) of this kind is high compared with that of carbonaceous solids, and thus melted ash does not wet or spread on the low-energy surface of the coke (7). This is confirmed by the observation (under the microscope) that coke particles appear to float on the surface of the glassy phase, as shown in the photomicrograph of Figure 5. The observed apparent contact angle between coke and the glassy phase varied from about 90 degrees to much more than that. This explains why so little coke is entrapped inside the melted ash.

We investigated the composition of the continuous or melt phase of the beads. Microscopic observations of polished sections (at higher magnification than shown in Figures 3 and 4) show the presence of crystals. The view in the photomicrograph of Figure 6 is typical, but occasional areas are found where the crystals are larger and comprise a larger fraction of the crystal-in-glass composite. Occasional particles of ferrous oxide and metallic iron have also been found and identified by measuring their reflectance. X-ray emission spectra of the crystals, obtained with a scanning electron microscope, indicated presence of iron and aluminum. Iron, aluminum, and silica were similarly identified as the major components of the matrix or continuous phase; titanium, potassium, and calcium were also detected in it.

It is well known that the fusibility of ash containing substantial amounts of iron (from pyrite in the original coal) depends on the oxidation-reduction potential of the atmosphere. The presence of occasional particles of metallic iron in the beads indicates that the atmosphere in at least some zones of the bed was reducing enough for reduction of ferrous oxide, although the product gas generally had too low a carbon monoxide-carbon dioxide ratio to expect such reduction. The phase diagram for the $\text{FeO-Al}_2\text{O}_3\text{-SiO}_2$ system in equilibrium with metallic iron is thus of interest for an understanding of the ash behavior.

The phase diagram of Osborn and Muan (6) for the $\text{FeO-Al}_2\text{O}_3\text{-SiO}_2$ system under this condition is shown in Figure 7. Note the narrow quadrilateral field for crystallization of iron cordierite, $2\text{FeO}\cdot 2\text{Al}_2\text{O}_3\cdot 5\text{SiO}_2$. The minimum liquidus temperature in the presence of hercynite ($\text{FeO}\cdot\text{Al}_2\text{O}_3$) and fayalite ($2\text{FeO}\cdot\text{SiO}_2$), at the lower left corner of the field, is $1990\pm 9^\circ\text{F}$. However, iron cordierite tends not to crystallize in the absence of seed crystals, and instead a metastable eutectic of fayalite, hercynite, and tridymite may form at $1963\pm 9^\circ\text{F}$ (5). In the presence of impurities, still lower liquidus temperatures may occur. Thus, Snow and McCaughy, working with mixtures prepared from clays containing impurities, found a liquidus temperature of 1778°F for this eutectic (9). However, no crystals typical of a eutectic were seen either by optical or scanning electron microscopy, nor was any fayalite detected by X-ray diffraction. Instead, it appears that a glass is formed when the melted ash cools.

Agglomerated Ash from FMC Char

The FMC char was much more reactive than the coke breeze, resulting in a lower bed temperature with comparable gas feed. On the other hand, more severe operating conditions (higher temperature or higher ash content of the bed) were required to obtain agglomerates large enough to be discharged automatically and in sufficient quantity to maintain the ash content of the bed in a steady state without periodic dumping. Steam had to be eliminated from the gas feed to obtain the required temperatures.

Agglomerated particles from two runs operating with FMC char as feed (Nos. 57 and 60) were examined. The feed for the first of these runs had been prepared from Illinois coal and that for the latter from Western Kentucky coal.

The agglomerated ash particles differed considerably from those produced from the coke breeze, being smaller and subangular instead of well-rounded. Particles from Run 60 are shown in Figure 2b with small beads from coke for comparison. In polished sections under the optical microscope, the clay of the coal ash appeared to be well-sintered, but no ferrous aluminum silicate was detected by X-ray emission in the scanning electron microscope. Instead, the iron appeared mostly in the form of ferrous sulfide and magnetite. In both feed chars, the iron appeared as ferrous sulfide; in the agglomerated ash from an early period of Run 57, some magnetite had appeared, but most of it was ferrous sulfide, much of it as separate particles. Some was occluded in the agglomerated

clay as dispersed, 1 to 10- μ m particles, and some had spread over the surface of the clay particles as shown in Figure 8. In the agglomerates from a later period of the run, much of the exposed iron, but not the occluded particles, had been converted to magnetite. In the agglomerated ash from a late period of Run 60, a portion of the magnetite on the outer zone of the particles had been reduced to wüstite (FeO). Rings of ferrous sulfide, similar in shape to those found on separate particles, were observed in the interior of the agglomerates. Formation and automatic discharge of these agglomerates occurred in Run 60 with a bed temperature of about 1950°F and an ash content of about 50% in the fluidized bed.

DISCUSSION

Differences in elemental composition among the three feed materials (Table 1) are probably not very significant in interpretation of the agglomeration process; however, analysis for acid-soluble iron indicated that a large part of the iron in the coke had already reacted with the clay minerals to form the acid-insoluble, low-melting ferrous aluminosilicate. (Pyrite also is insoluble in hydrochloric acid but is decomposed or oxidized in the preparation of the coke and char. Soluble iron compounds occluded in sintered clay also do not dissolve.)

Table 1. PROPERTIES OF ASH IN COKE AND CHAR FEEDS

Elemental Composition, wt %	Coke	FMC Char	
		From Ill. Coal	From Ky. Coal
SiO ₂	47.1	35.7	39.9
Al ₂ O ₃	20.8	17.5	23.4
Fe ₂ O ₃	18.9	24.1	24.1
TiO ₂	0.81	0.88	0.51
CaO	3.25	3.50	0.43
MgO	1.01	0.85	0.74
Na ₂ O	0.54	4.03	0.60
K ₂ O	1.72	2.48	0.65
SO ₃	2.26	5.15	1.95
Total	96.4	93.4	92.3
Acid-Soluble Iron, % of total iron	47	98	97
Ash Fusibility, °F			
Reducing Atmosphere			
IT	2085	1780	2005
ST	2155	1950	2050
HT	2230	1980	2080
FT	2440	2160	2340
Oxidizing Atmosphere			
IT	2510	2215	2475
ST	2630	2300	2520
HT	--	2360	2540
FT	--	2500	2560

Thus, two different modes of ash agglomeration are indicated, namely, iron oxide fluxing (formation of molten ferrous aluminum silicate), and, under more severe conditions, clay sintering. Possibly the presence of relatively low-melting (and thus prone to sintering) ferrous sulfide (mp 2180°F) on the exterior of clay particles may have aided in their agglomeration.

Prediction of the performance that will be obtained with other types of feed is uncertain. The form of the iron in the feed is obviously important; iron in hydrogasification residue, for example, is likely to have been converted to ferrous oxide and would thus be in a much readier form to react with and flux the clay than it is in char. This may also be the case even with raw coal as the feed, because a gasification atmosphere has a higher oxidation potential than a pyrolysis atmosphere does.

ACKNOWLEDGMENTS

This work was conducted as part of the HYGAS[®] coal gasification program jointly sponsored by the United States Energy Research and Development Administration (ERDA) and the American Gas Association. This program is under the technical direction of Dr. C. Lowell Miller and Mr. Stephen C. Verikios of ERDA and Dr. Ab Flowers of the American Gas Association.

REFERENCES

1. ASTM 1975 Annual Book of ASTM Standards, Part 26 - Gaseous Fuels; Coal and Coke; Atmospheric Analysis, D 2797, "Preparing Coal Samples for Microscopical Analysis by Reflected Light." Philadelphia: American Society for Testing and Materials, 1975.
2. Boar, P. L. and Ingram, L. K., "Comprehensive Analysis of Coal Ash and Silicate Rocks by Atomic-Absorption Spectrophotometry by a Fusion Technique," Analyst (London) 95 (1127), 124-30 (1970).
3. Cameron, E. N., Ore Microscopy. New York: John Wiley, 1961.
4. Mason, D. M. and Schora, F. C., Jr., "Coal and Char Transformation in Hydrogasification," Adv. Chem. Ser. No. 69, 18-30 (1967).
5. Muan, A., "Phase Equilibrium Relationships at Liquidus Temperatures in the System FeO-Fe₂O₃-Al₂O₃-SiO₂," J. Amer. Ceram. Soc. 40, 420-31 (1957).
6. Osborn, E. F. and Muan, A., in Levin, E. M., Robbins, C. R. and McMurdie, H. F., Eds., Phase Diagrams for Ceramists, 241. Columbus: The American Ceramic Society, 1964.
7. Raask, E., "Slag-Coal Interface Phenomena," J. Eng. Power 88 (No. 1), 40-44 (1966).
8. Sandstrom, W. A., Rehmat, A. G. and Bair, W. G., "The Gasification of Coal Chars in a Fluidized-Bed Ash-Agglomeration Gasifier." Paper presented at the A. I. Ch. E. 69th Annual Meeting, Chicago, November 28 - December 2, 1976.
9. Snow, R. B. and McCaughy, W. J., "Equilibrium Studies in the System FeO-Al₂O₃-SiO₂," J. Amer. Ceram. Soc. 25, 151-60 (1942).

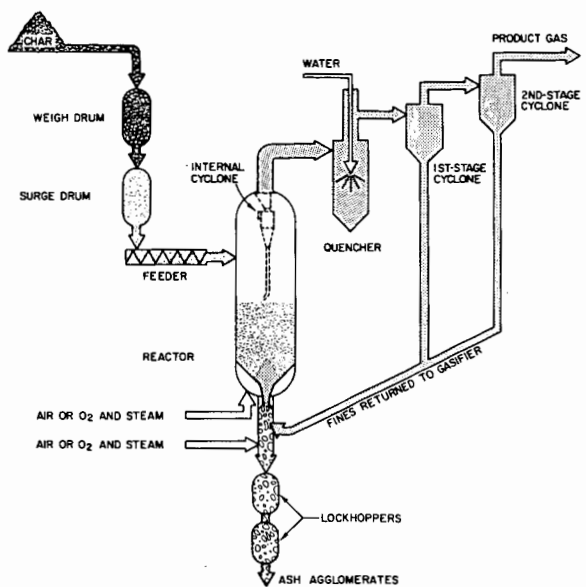


Figure 1. SCHEMATIC DIAGRAM OF ASH-AGGLOMERATING GASIFIER

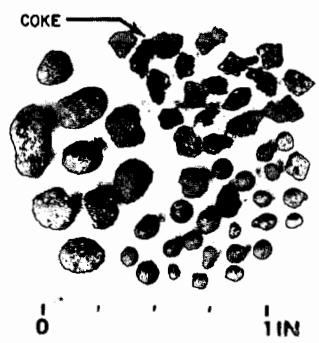


Figure 2a.
ASH AGGLOMERATES FROM
COKE, WITH COKE PARTICLES



Figure 2b. ASH AGGLOMERATES FROM
FMC CHAR (Left), AND COKE (Right)

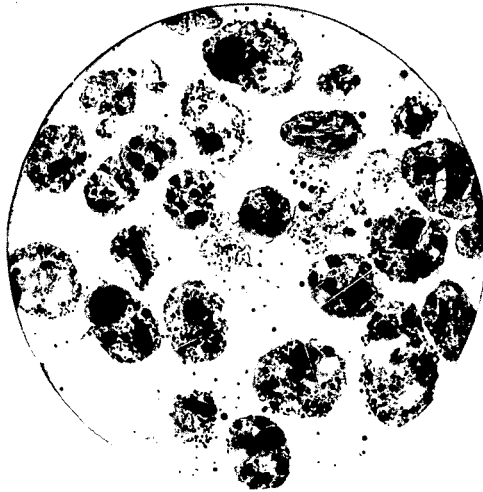


Figure 3. AGGLOMERATED ASH BEADS
FROM COKE - VERTICAL ILLUMINATION

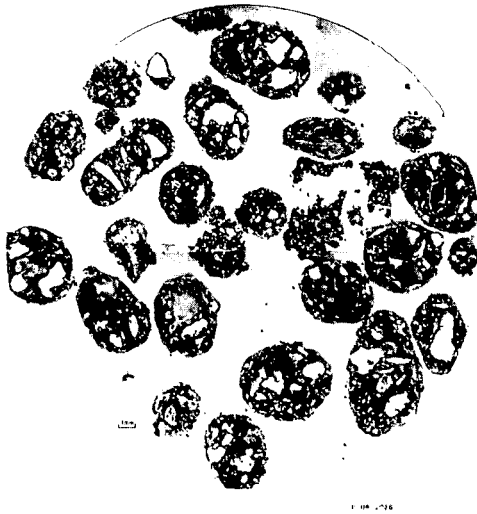


Figure 4. AGGLOMERATED ASH BEADS
FROM COKE - OBLIQUE ILLUMINATION

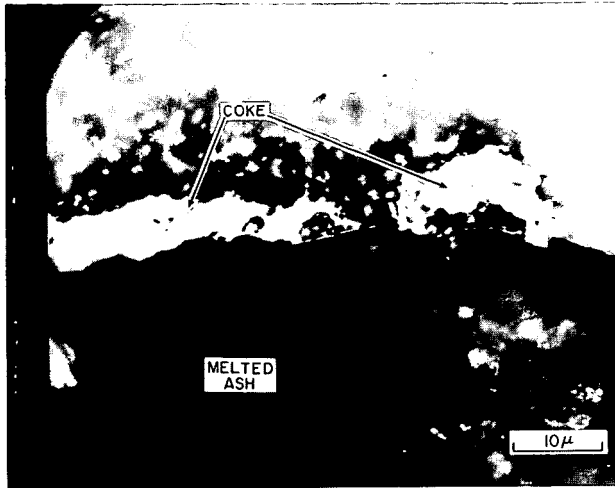


Figure 5. COKE PARTICLES ON SURFACE OF MELTED AND RESOLIDIFIED ASH OBSERVED BY OPTICAL MICROSCOPE WITH OIL IMMERSION

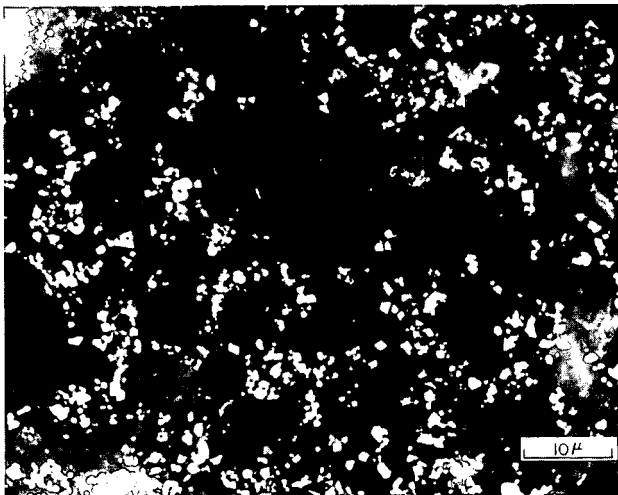


Figure 6. CRYSTALS OF HERCYNITE ($\text{FeO} \cdot \text{Al}_2\text{O}_3$) IN MELTED AND RESOLIDIFIED ASH OBSERVED BY OPTICAL MICROSCOPE WITH OIL IMMERSION

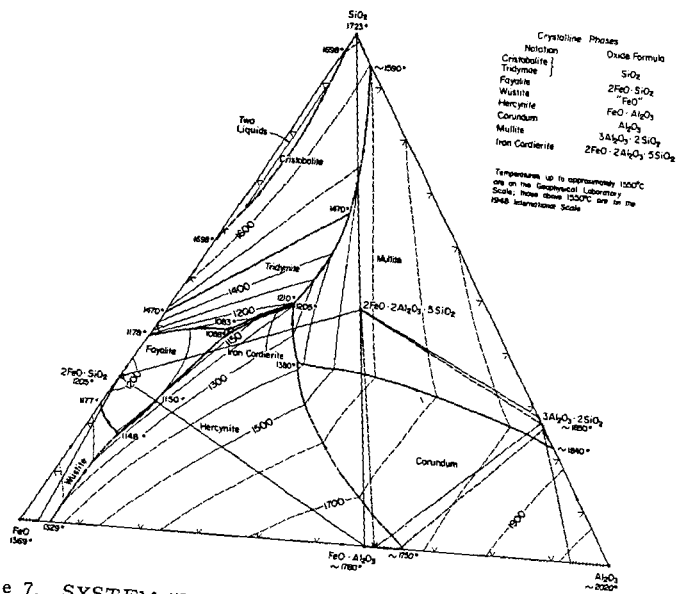


Figure 7. SYSTEM "FeO"-Al₂O₃-SiO₂; COMPOSITE, BY WEIGHT (Oxide Phases in Equilibrium With Metallic Iron)(6)

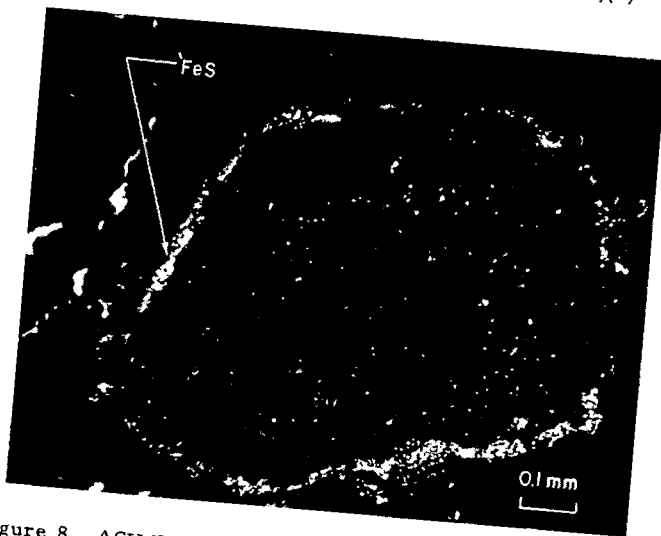


Figure 8. ASH PARTICLES FROM FMC CHAR SHOWING A COATING OF FERROUS SULFIDE ON SINTERED CLAY

Petrochemistry of Coal Ash Slags. 1. Formation of Melilite and a High Temperature Glass from a Calcium-Rich, Silica-Deficient Slag.

H. H. Schobert,^{1/} D. L. Barbie,^{2/} O. D. Christensen,^{3/} and F. R. Karner^{4/}

Grand Forks Energy Research Center
Box 8213, University Station
Grand Forks, ND 58202
and
Department of Geology
University of North Dakota
Grand Forks, ND 58202

The Grand Forks Energy Research Center (GFERC) of the Energy Research and Development Administration is conducting pilot plant studies of a fixed-bed slagging coal gasification process. The pilot plant was originally operated from 1958-1965 by the Bureau of Mines. The design and operation of the gasifier and the Bureau of Mines test results have been documented (1,2). Recent papers (3,4) have described the program objectives for the reactivated plant and have presented some preliminary results.

A schematic diagram of the gasifier is shown in Figure 1. Lignite or subbituminous coal is reacted with steam and oxygen at pressures to 27 atmospheres psig and at hearth zone temperatures exceeding 1650° C. A gas mixture is produced of which 90% is carbon monoxide and hydrogen at 2:1 ratio and the balance is composed of methane, carbon dioxide, and nitrogen. The hearth zone temperatures are maintained sufficiently high to cause melting of the ash. The molten slag drains into a water quench bath through a taphole in the hearth. Maintaining a steady flow of slag is crucial to the successful operation of the gasifier, since a build-up of slag on the hearth or a plug forming in the taphole will result in a premature shutdown of the test.

The petrochemistry of the slag is of considerable importance as a factor in hearth section design. Refractory selection will depend in part upon the chemical relationship between slag constituents and the refractories. If a phase transformation in the slag should produce a liquid having a composition well outside the design specifications, a rapid chemical degradation of the refractory structures could occur. The temperature dependence of slag viscosity is a function of slag composition. Since design of slag discharge orifices will be influenced in part by the expected viscosity range, viscosity changes caused by corresponding composition changes could alter slag flow characteristics.

Additional interest in slag petrochemistry arises from a similarity of slag compositions to naturally-occurring silicate melts. Thus the slagging operations in the gasifier can provide opportunities for studies of igneous rock petrology.

During operation, the slag is removed from the gasifier by periodically discharging the slag lock. The discharged slag is recovered as black, glassy granules (Fig. 2). In some tests the slag has been found to contain structures of

^{1/} Research Chemist, Grand Forks Energy Research Center.

^{2/} Physical Science Aide, Grand Forks Energy Research Center.

^{3/} Assistant Professor of Geology, University of North Dakota.

^{4/} Professor of Geology, University of North Dakota.

unusual or atypical appearance. Samples of these are retained for detailed chemical and petrographic analysis. It is of particular concern to identify the phases formed, to determine or suggest the mechanism of the phase separation, and to predict the effect on such parameters as refractory attack, slag viscosity, and heat transfer.

The current series of tests in the GFERC gasifier uses lignite from the Indianhead mine of the North American Coal Company near Zap, North Dakota. Slag analyses are done using x-ray fluorescence. The analysis of the bulk slag varies slightly from run to run. Table 1 shows the slag analysis for a recent test and the range of observed values.

TABLE 1. Product Slag Analysis, Indianhead Lignite.

<u>Oxides</u>	<u>Wt.,%</u>	<u>Range, %</u>
SiO ₂	39.5	31.1 - 39.7
Al ₂ O ₃	13.6	11.8 - 13.6
Fe ₂ O ₃	11.0	4.4 - 11.4
TiO ₂	0.7	0.4 - 0.7
P ₂ O ₅	0.3	0.3 - 0.6
CaO	17.9	17.9 - 33.7
MgO	5.3	5.3 - 7.4
Na ₂ O	6.6	0.1 - 10.5
K ₂ O	1.0	0.6 - 1.0
SO ₃	4.1	1.9 - 4.1
TOTAL	100.0	

The composition is similar to that of a calcium-rich pyroxene.

Figure 3 shows a specimen of two-layered nodules recovered from the product slag of an early test (No. RA-4) in the current program. Table 2 shows the results of analysis of the inner and outer layers of the nodules, as well as the analysis of a bulk sample of the slag.

TABLE 2. Analyses of Regions of Indianhead Slag Nodules, Test RA-4

	<u>Weight Percent</u>		
	<u>Inner Layer</u>	<u>Outer Layer</u>	<u>Bulk Sample</u>
SiO ₂	65.0	36.6	38.2
Al ₂ O ₃	19.3	13.6	12.7
Fe ₂ O ₃	5.8	13.0	8.0
TiO ₂	0.9	0.7	0.6
P ₂ O ₅	0.1	0.4	0.5
CaO	1.7	20.6	24.3
MgO	2.6	5.6	6.4
Na ₂ O	1.4	5.8	3.5
K ₂ O	2.9	0.8	0.9
SO ₃	0.2	3.0	3.0
TOTAL	99.9	100.1	98.1

A thin section of one of these nodules is shown in Figure 4. Optical and x-ray diffraction study shows that the inner material is a vesicular glass with a small amount of disseminated quartz grains or fragments. The vesicles vary in size across the thin-sectioned chips, typically occurring in zones of smaller (0.01 mm) and larger (0.04 mm) approximate average diameter. In addition to the vesicles, numerous similar, spherical structures with pale tan color are present. These often contain or partly contain quartz grains. The outer layer of the nodules is very similar to the original slag.

Figure 5 shows a portion of a SiO₂-CaO-MgO ternary slice through the SiO₂-CaO-MgO-Al₂O₃ quaternary system, at 15 pct Al₂O₃. (Points are plotted on the basis of SiO₂ + CaO + MgO + Al₂O₃ = 100 pct). The composition of the inner layer lies in the cristobalite field, while both the outer layer and bulk slag compositions lie in the pyroxene field. The fact that crystallization of the inner layer was not more pronounced is very likely due to undercooling, since reported (5) slag discharge temperatures of 2300° F (1260° C) are less than 100° C above the fluid temperature of Indianhead slag.

The three-layered nodules were recovered from the slag in a more recent test (RA-7). The analysis of each layer is given in Table 3, along with an analysis of the bulk slag.

TABLE 3. Analyses of Regions of Indianhead Slag Nodules, Test RA-7

	<u>Inner Layer</u>	<u>Middle Layer</u>	<u>Outer Layer</u>	<u>Bulk Sample</u>
SiO ₂	36.6	37.8	39.2	33.1
Al ₂ O ₃	10.2	8.9	12.5	13.1
TiO ₂	0.3	0.3	0.5	0.5
P ₂ O ₅	0.5	0.5	0.5	0.6
CaO	40.5	38.7	31.1	22.6
MgO	7.9	9.5	6.8	5.4
Na ₂ O	0.3	0.5	1.2	6.1
K ₂ O	0.3	0.3	0.6	0.8
SO ₃	3.1	2.5	1.4	2.4
Fe ₂ O ₃	0.2	1.0	6.1	11.4
TOTAL	99.9	100.0	99.9	96.0

Thin section photographs of a three-layered nodule are shown in Figures 6 and 7. Optical and x-ray diffraction data show that the inner layers contain abundant melilite while the outer core is a glass. Melilite occurs as two types of clusters of radiating, zoned crystals. One type has zoning produced by dark, reddish cores, probably resulting from abundant iron-rich inclusions and exhibits a well developed dendritic intergrowth texture, probably from quenching. The second type of melilite has zoning shown by birefringence characteristics, probably from oscillatory or reverse chemical zoning and subhedral to euhedral crystal form.

In both cases these phase transformations can be related to temperature fluctuations in the gasifier hearth. Hearth zone temperatures are measured by a thermocouple mounted on the bottom of the hearth plate, and another in the gasifier wall approximately 5-1/2 feet above the hearth. Figures 8 and 9 show the two temperatures as a function of time for tests RA-4 and RA-7, as well as test RA-8, in which no slag phase separation was observed. Temperature data from RA-4 and RA-7 show sharp fluctuations, whereas the data from RA-8 show relatively stable temperatures.

The slag-refractory chemistry was found not to be significantly affected by either phase transformation described here. The slags have been characterized by calculating the base to acid ratio:

$$B/A = \frac{CaO + MgO + Na_2O + K_2O + Fe_2O_3}{SiO_2 + Al_2O_3 + TiO_2}$$

In the case of glass formation, the bulk slag has a basicity/acidity ratio of 0.84, while the liquid phase which would remain after formation of the glass nodules has a value of 0.90 (calculated from the analysis of the outer layer of the nodules). The corresponding values for the melilite formation are, respectively, 0.99 and 0.88. Neither situation represents a drastic change in slag basicity. Accelerated chemical degradation of hearth zone refractories is therefore an unlikely consequence of these phase transformations.

Changes in slag viscosity were estimated by calculating viscosities from a modified form of the Watt-Fereday equation (7),

$$\log \eta = 10^7 M / (T-150)^2 + C$$

where M and C are empirical constants which are functions of slag composition, the viscosity in poise, and the temperature in degrees Centigrade. Preliminary results from current GFERC research on adapting the Watt-Fereday equation to lignite slags were used to estimate order-of-magnitude viscosity changes. Viscosities were calculated from the bulk slag analysis and from the analysis of the outer layer of the nodules. Massive formation of melilite from Indianhead slag would leave a residual liquid having a calculated viscosity of 125 poise at 1350° C, while the calculated viscosity of the bulk slag is only 8 poise.

The change in slag viscosity will also affect hearth zone heat transfer relationships. For example, the calculation of the heat transfer coefficient between the slag and hearth plate is dependent upon the Grashof and Prandtl numbers for the flowing slag, both of which are functions of viscosity (8).

The results of this study show that the characteristics of the coal ash slag can be affected by temperature fluctuations in the gasifier hearth. Chemical, flow, and heat transfer behavior are all susceptible to change as a result.

REFERENCES

1. G.H. Gronhovd, A.E. Harak, W.R. Kube, and W.H. Oppelt. "Design and Initial Operation of a Slagging, Fixed-Bed, Pressure Gasification Pilot Plant." U.S. Bureau of Mines RI 6084 (1962).
2. G.H. Gronhovd, A.E. Harak, M.M. Fegley, and D.E. Severson. "Slagging Fixed-Bed Gasification of North Dakota Lignite at Pressures to 400 psig." U.S. Bureau of Mines RI 7408 (1970).
3. R.C. Ellman and B.C. Johnson. "Slagging Fixed-Bed Gasification at the Grand Forks Energy Research Center." Presented at the Eighth Synthetic Pipeline Gas Symposium, Chicago, IL, October 1976.

4. R.C. Ellman and H.H. Schobert. "Pilot Plant Operation of a Fixed-Bed Slagging Gasifier." Presented at the National Meeting of the American Chemical Society, New Orleans, LA, March 1977.
5. G.H. Gronhovd. "Quarterly Technical Progress Report, April-June, 1976." ERDA Report GPERC/QTR-76/4 (1976).
6. B. Mason. "Principles of Geochemistry." Second Ed., John Wiley and Sons, Inc, New York, NY 1958.
7. J.D. Watt and F. Fereday. "The Flow Properties of Slags Formed From the Ashes of British Coals: Part 1: Viscosity of Homogeneous Liquid Slags in Relation to Slag Composition." J. Inst. Fuel, 42, 99 (1969).
8. C.O. Bennett and J.E. Myers. "Momentum, Heat, and Mass Transfer." Second Ed., McGraw-Hill Book Co., New York, NY 1974.

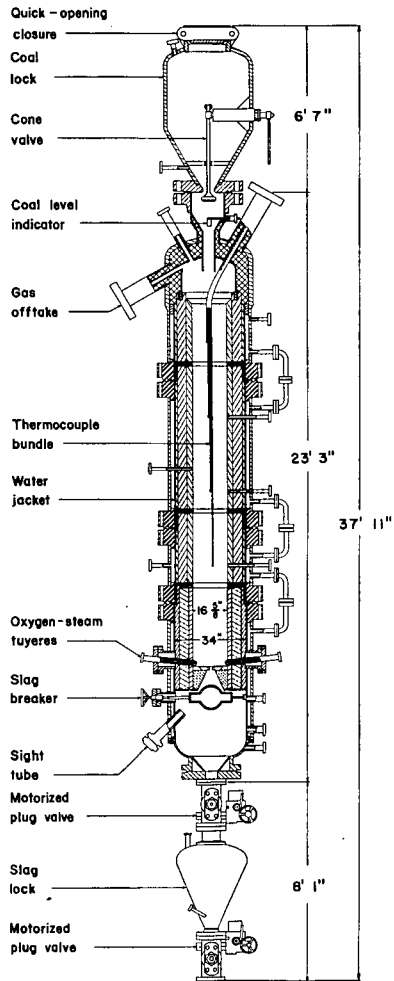


Figure 1. GFERC Gasifier



Figure 2. Typical Discharged Slag



Figure 3. Two-layered Slag Nodules

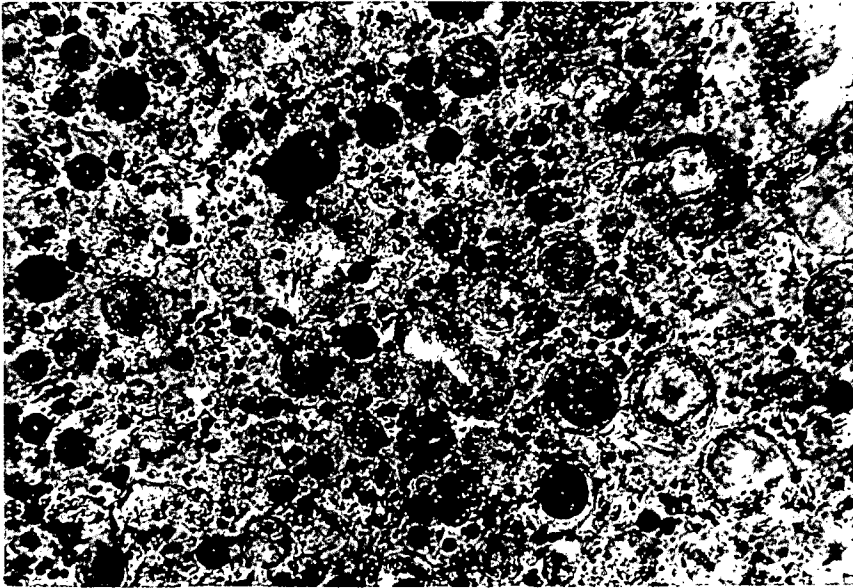


Figure 4. Thin section photograph of glassy part of two-layered nodule, showing two types of spherical structures. Photo taken using partly crossed polars; field of view, 0.7 mm.

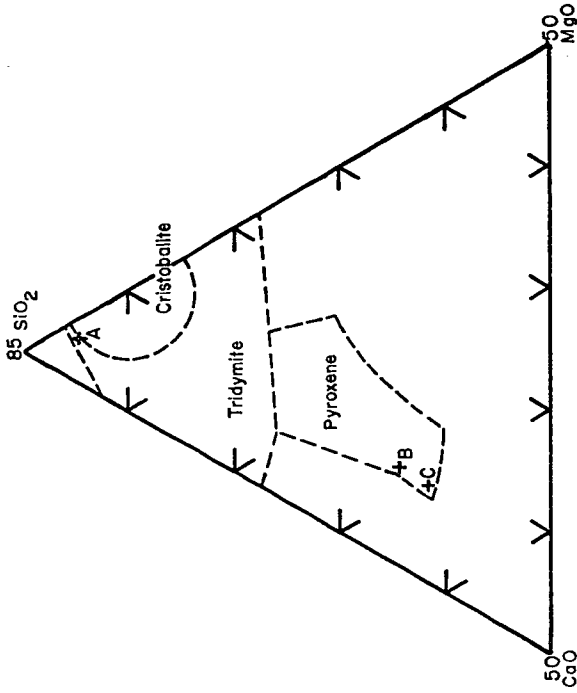


Figure 5. SiO_2 -CaO-MgO Ternary at 15% Al_2O_3

A=Glass, B=Outer Layer of Nodule, C= Bulk Slag Composition

Figure 5. SiO_2 -CaO-MgO Ternary slice of SiO_2 -CaO-MgO- Al_2O_3 system. (15% Al_2O_3).

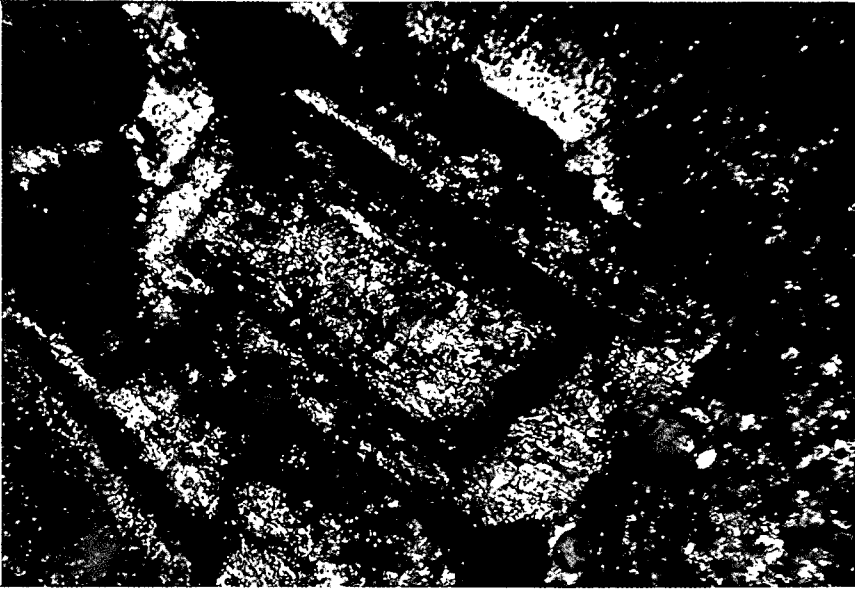


Figure 7. Melilite in three-layered nodules. Crystal with chemical zoning shown by birefringence characteristics. Photo taken with crossed polars. Field of view, 1.2 mm.

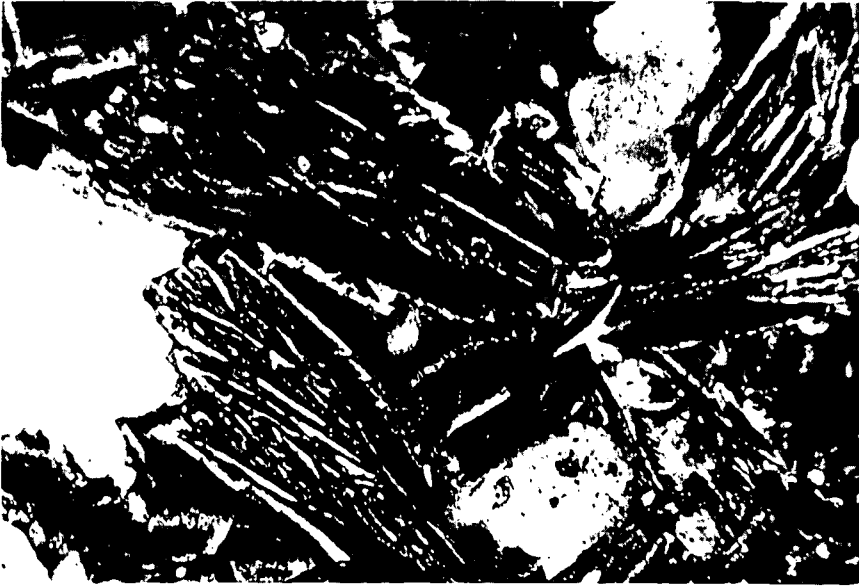


Figure 6. Melilite in three-layered nodules. Inter-growth of dendritic crystals with iron-rich cores. Photo taken in plane polarized light. Field of view, 3 mm.

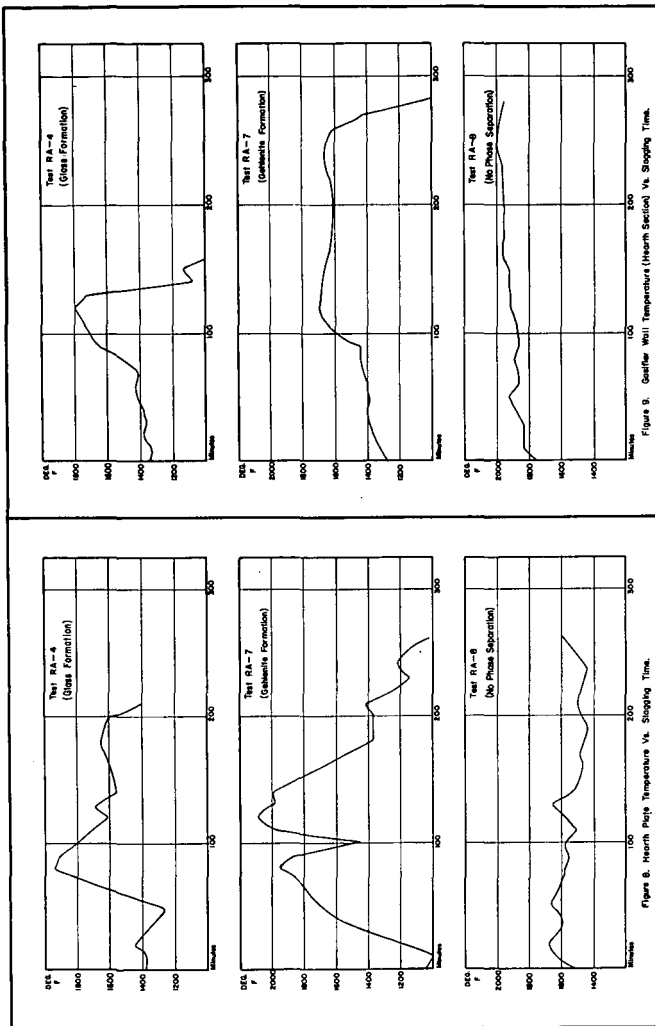


Figure 8. Guller Well Temperature (Warm Section) Vs. Stopping Time.

Figure 9. Harsh Pipe Temperature Vs. Stopping Time.